

SCNet: Training Inference Sample Consistency for Instance Segmentation

Thang Vu, Haeyong Kang, Chang D. Yoo

Department of Electrical Engineering
Korea Advanced Institute of Science and Technology
{thangvubk,haeyong.kang,cd.yoo}@kaist.ac.kr

Abstract

Cascaded architectures have brought significant performance improvement in object detection and instance segmentation. However, there are lingering issues regarding the disparity in the Intersection-over-Union (IoU) distribution of the samples between training and inference. This disparity can potentially exacerbate detection accuracy. This paper proposes an architecture referred to as Sample Consistency Network (SCNet) to ensure that the IoU distribution of the samples at training time is close to that at inference time. Furthermore, SCNet incorporates feature relay and utilizes global contextual information to further reinforce the reciprocal relationships among classifying, detecting, and segmenting sub-tasks. Extensive experiments on the standard COCO dataset reveal the effectiveness of the proposed method over multiple evaluation metrics, including box AP, mask AP, and inference speed. In particular, while running 38% faster, the proposed SCNet improves the AP of the box and mask predictions by respectively 1.3 and 2.3 points compared to the strong Cascade Mask R-CNN baseline. Code is available at <https://github.com/thangvubk/SCNet>.

1 Introduction

In recent years, instance segmentation has received considerable attention for its applications in autonomous driving (Neven et al. 2018; Zhang, Fidler, and Urtasun 2016), robotics (Danielczuk et al. 2019; Pathak et al. 2018), surveillance (Mao et al. 2018; Zhang et al. 2018), and other vision tasks (Kim et al. 2019, 2020). Given an image, instance segmentation aims to predict class labels and instance masks for objects of interest at pixel-level. Achieving an accurate and robust instance segmentation in a real-world environment is challenging: object occlusion, deformation, and scale changes are of concern.

State-of-the-art instance segmentation methods attempt to benefit from high performing object detectors, where the predicted boxes are segmented using a fully convolutional network (Long, Shelhamer, and Darrell 2015), such as Mask R-CNN (He et al. 2017), and PANet (Liu et al. 2018). For accurate object detection, Cascade R-CNN (Cai and Vasconcelos 2018) has been recently proposed, showing significant

performance improvement. It consists of a sequence of detectors that progressively refine the box predictions to obtain accurate localization at the final detection stage. The capability of this detector has been extended with the addition of the mask branches for performing instance segmentation. This architecture is referred to as the Cascade Mask R-CNN (Cai and Vasconcelos 2019), which shows significant improvement compared to non-cascade ones. Although having better performance compared to non-cascade methods, Cascade Mask R-CNN still exhibits inconsistency in training and inference sample distribution. At training time, the outputs of all the box stages are used for mask predictions; however, at inference time only the output of the last box stage is used for mask predictions. It has been shown in (Cai and Vasconcelos 2018) that the box stages produce different sample distributions since they are trained with different Intersection over Union (IoU) thresholds. Such a mismatch between training and inference sample distribution will potentially worsen the performance.

This paper proposes an architecture referred to as Sample Consistency Network (SCNet) that ensures the IoU distribution of the samples at training time to be close to that at inference time. To this end, only the outputs of the last box stage are used for mask predictions at both training and inference. Figure 1 shows the IoU distribution of the samples going to the mask branch at training time with/without sample consistency compared to that at inference time. The COCO (Lin et al. 2014) train and val splits are used for training and inference, respectively. When sample consistency is not ensured, nearly half of the training samples (49.1%) are at a low IoU region ($\text{IoU} \leq 0.75$), which are much larger than that of training with sample consistency (34.2%) and inference (38.5%). Overall, training with sample consistency produces closer IoU distribution between training and inference compared to that of training without sample consistency.

Instance segmentation requires synergy among the three sub-tasks: detecting, classifying, and segmenting objects. To further reinforce the reciprocal relationships among sub-tasks, *feature relay* and *global context* are proposed. It is well-known that joint training of closely related tasks can improve the overall performance (He et al. 2017; Chen et al. 2019a). For instance, adding an extra mask branch to a detector improves the detection performance, although there is no direct information flow between the box and mask

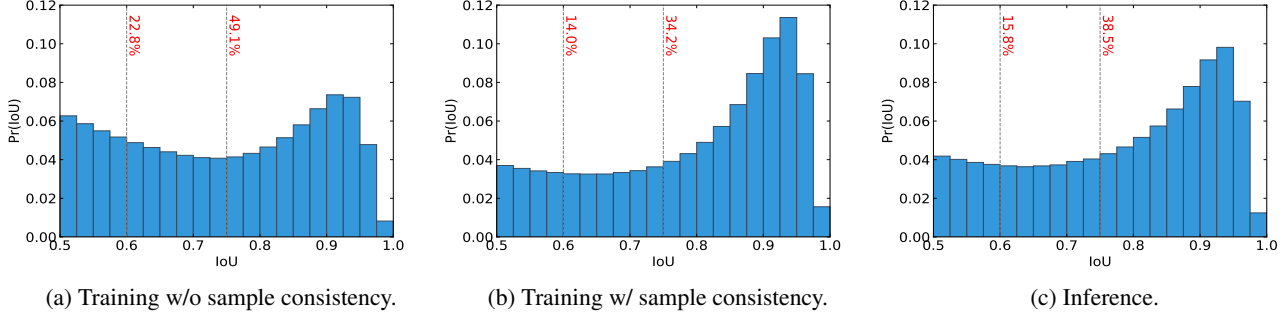


Figure 1: IoU distribution in training with/without sample consistency and inference. The red numbers show the percentages of the samples having IoU less than the corresponding threshold.

branches (He et al. 2017). It shows that the “implicit” mutual information between detection and segmentation improves the overall performance. This paper takes this concept a step further and introduces an “explicit” connection linking the output of the box branch to the input of the mask branch to elevate mutual information between the outputs of the two branches that ultimately enhance segmentation performance. This process is referred to as feature relay.

Common methods for detection and segmentation are performed in a region-wise manner, where the prediction is made based on features extracted from a small region by the pooling layer, such as RoIAlign (He et al. 2017). These layers serve as a hard attention mechanism that enables the detector to focus on the relevant region of the image. However, in a number of cases, objects are visually ambiguous when they stand alone. To overcome this limitation, SCNet relies on a global context branch to provide each object context prior for the final prediction.

2 Related Work

Instance Segmentation. There are two main streams in instance segmentation: proposal-based and proposal-free methods. In proposal-based methods, conventional detectors (Girshick 2015; Vu et al. 2019) generate region proposals, then instance masks are predicted within the proposed regions. DeepMask (Pinheiro, Collobert, and Dollár 2015), SharpMask (Pinheiro et al. 2016), and InstanceFCN (Dai et al. 2016) learn to produce segment candidates instead of bounding boxes as proposals. Li *et al.* extend InstanceFCN and propose FCIS for instance segmentation by introducing position-sensitive score maps (Li et al. 2017). In (Dai, He, and Sun 2016), a multi-task cascade is proposed, where the output of a sub-task is used as input of the next sub-task. He *et al.* present Mask R-CNN (He et al. 2017) by appending a segmentation branch in parallel to the detection branch of Faster R-CNN (Ren et al. 2015), showing promising results. Liu *et al.* extend Mask R-CNN and propose PANet (Liu et al. 2018), which aims to enhance the feature hierarchy by adding a bottom-up path into the standard FPN (Lin et al. 2017). Recent advanced methods (Cai and Vasconcelos 2019; Chen et al. 2019a) extend the multi-stage detector Cascade R-CNN (Cai and Vasconcelos 2018) to produce

high-quality instance segmentation.

In proposal-free methods, object instances are directly identified without proposals. In (Zhang, Fidler, and Urtasun 2016; Zhang et al. 2015), local instance labels are predicted and integrated with a Markov Random Field (MRF) to obtain globally consistent instance labels. In (Arnab and Torr 2016), a semantic segmentation map is first predicted, then instances are identified, relying on a Conditional Random Field (CRF) model. Bai and Urtasun propose a watershed transform network to obtain an energy map, then derive instances based on the energy levels (Bai and Urtasun 2017). In (Liu et al. 2017), a sequence of networks is designed to predict horizontal and vertical object breakpoints, which are then merged to produce object instances. In (Tian, Shen, and Chen 2020), a dynamic instance-aware network is proposed to replace ROI operation, leading to a compact and fast model. Xie *et al.* propose PolarMask, which formulates the instance segmentation problem as instance center classification and dense distance regression in a polar coordinate (Xie et al. 2020). Wang *et al.* propose SOLO which directly predicts mask instances by assigning categories to each pixel within an instance according to the instances location and size (Wang et al. 2020). Overall, the proposal-free methods are simple and fast; however, proposal-based methods are generally more accurate.

Multi-stage Instance Segmentation. In proposal-based approach, benefiting from the high-performing multi-stage detector, Cascade Mask R-CNN (Cai and Vasconcelos 2019) shows improvement when compared to non-cascade methods for instance segmentation. Recently, Chen *et al.* (Chen et al. 2019a) have extended Cascade Mask R-CNN and propose HTC to improve segmentation by constructing mask information flow through stages and introducing a semantic branch. Although showing improvements compared to non-cascade methods, Cascade Mask R-CNN and HTC show limitation of inconsistency in training and inference sample distribution and the requirement of multi-stage mask predictions, which is not computationally efficient. The proposed SCNet differs from previous methods in that it ensures the sample consistency between training and testing time. Sample consistency is optimized to not only improve the accuracy but also improve the inference speed by avoiding the

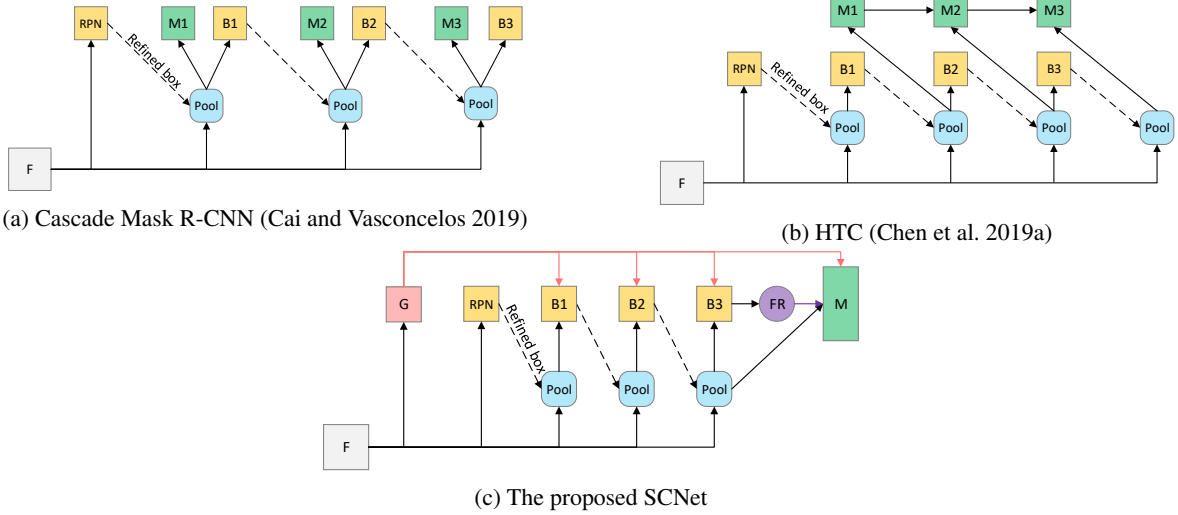


Figure 2: Architecture of cascade approaches: (a) Cascade Mask R-CNN. (b) Hybrid Task Cascade (HTC). (c) the proposed SCNet. Here, “F”, “RPN”, “Pool”, “B”, “M”, “FR” and “G” denote image features, Region Proposal Network (Ren et al. 2015), region-wise pooling, box branch, mask branch, feature relay, and global context branch, respectively. It is noted that each box branch performs both box regression and classification. Additionally, the semantic branch (Chen et al. 2019a), which is not shown for a neat presentation, is applied to all cascade models for a fair comparison

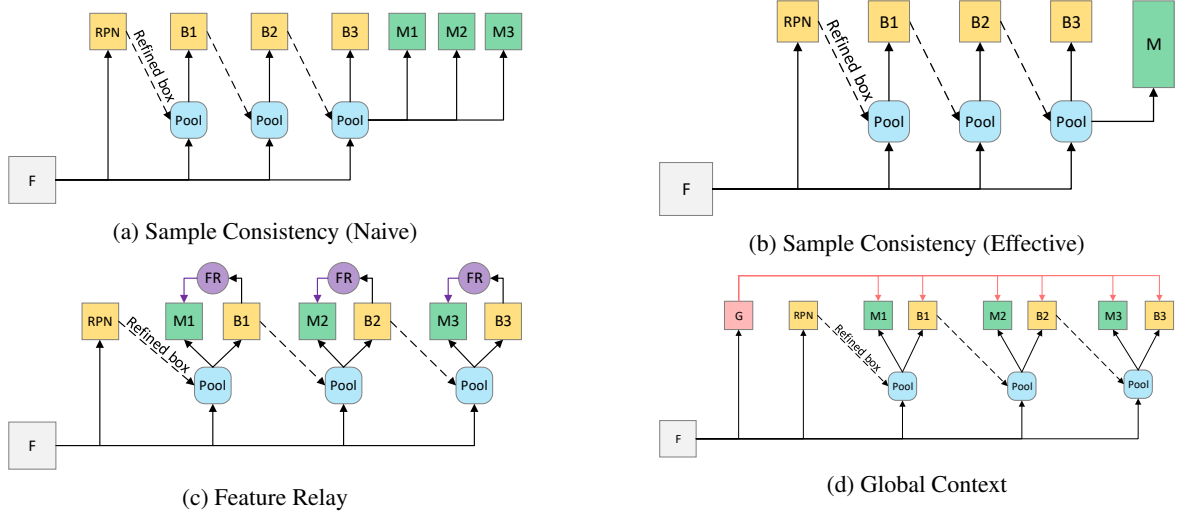


Figure 3: Individual components of the proposed SCNet, which are applied to the baseline Cascade Mask R-CNN.

repetition of expensive operations, including mask RoI feature extraction, feature upsampling, and mask prediction. The performance of SCNet is also further improved with the incorporation of feature relay and global context information. Feature relay creates the information flow between box and mask branch. Global context provides individual objects with context prior for final prediction. The crucial difference between the proposed global context branch with previous methods in object detection (Wang et al. 2018; Cao et al. 2019; Qiao, Chen, and Yuille 2020) is that these methods incorporate global context in the backbone at pixel level meanwhile the proposed method incorporates global context in the detector stages (R-CNN) at instance-level. It is nontrivial

to improve detection performance in R-CNN by global context since simply applying Global Convolution Network (Peng et al. 2017) does not show performance gain (Chen et al. 2019a). It is expected that the proposed global context branch is complemented with backbone-based global context since they improve different parts of the detector.

3 Cascade Architectures

3.1 Cascade Mask R-CNN

Cascade Mask R-CNN is the combination of the high-performing detector Cascade R-CNN and the popular segmentation method Mask R-CNN. Figure 2a illustrates the

architecture of a 3-stage Cascade Mask R-CNN. Mathematically, Cascade Mask R-CNN can be formulated as follows.

$$\begin{aligned} \mathbf{x}_t^{box} &\leftarrow \mathcal{P}(\mathbf{x}, \mathbf{b}_{t-1}), \quad \mathbf{b}_t \leftarrow \mathcal{B}_t(\mathbf{x}_t^{box}), \\ \mathbf{x}_t^{mask} &\leftarrow \mathcal{P}(\mathbf{x}, \mathbf{b}_{t-1}), \quad \mathbf{m}_t \leftarrow \mathcal{M}_t(\mathbf{x}_t^{mask}). \end{aligned} \quad (1)$$

Here, \mathbf{x} is the feature maps from a convolutional backbone network. At stage t , a region-wise pooling operator \mathcal{P} extracts box features \mathbf{x}_t^{box} and mask features \mathbf{x}_t^{mask} based on the backbone features and predicted boxes (or region proposals) at the previous stage \mathbf{b}_{t-1} . The predicted boxes \mathbf{b}_t and masks \mathbf{m}_t are derived from the box branch \mathcal{B}_t and mask branch \mathcal{M}_t , respectively.

Even though performing better than other non-cascade methods, Cascade Mask R-CNN exhibits two main limitations in its architecture as follows. First, the mask predictions at training and inference come from different distributions. At training time, the outputs of all the box stages are used for mask predictions; however, at inference time only the output of the last box stage is used for mask predictions. This is because at inference time, the mask ensemble requires the mask predictions upon the same ROI locations. Although using multiple box stages for mask prediction improves the sample diversity (Cai and Vasconcelos 2018), the proposed SCNet shows that making the training sample distribution close to that of inference further improves the performance. Second, the mask branches are isolated without direct connections, and inaccurate mask predictions are made on intermediate noisy boxes, as shown in Figure 2a. The effectiveness of Cascade Mask R-CNN mainly stems from the high-performing detector and the ensemble of multiple isolated mask branches.

3.2 Hybrid Task Cascade

To alleviate the problems of Cascade Mask R-CNN, Hybrid Task Cascade (HTC) (Chen et al. 2019a) introduces interleaved execution between box and mask branches and direct information flow through the mask branches. The pipeline of HTC can be described as follows.

$$\begin{aligned} \mathbf{x}_t^{box} &\leftarrow \mathcal{P}(\mathbf{x}, \mathbf{b}_{t-1}), \quad \mathbf{b}_t \leftarrow \mathcal{B}_t(\mathbf{x}_t^{box}), \\ \mathbf{x}_t^{mask} &\leftarrow \mathcal{P}(\mathbf{x}, \mathbf{b}_t), \quad \mathbf{m}_t \leftarrow \mathcal{M}_t(\mathcal{F}(\mathbf{x}_t^{mask}, \mathbf{m}_{1:t-1})). \end{aligned} \quad (2)$$

Here, HTC performs interleaved execution to leverage the observation that the boxes are more accurate after box regression, where the segmentation step is based on the output of detection step \mathbf{b}_t instead of \mathbf{b}_{t-1} . Besides, there is a direct information flow through the mask branches. In concrete, the current backbone features \mathbf{x}_t^{mask} are combined with the accumulated mask features from the previous stages $\mathbf{m}_{1:t-1}$ by a fusion operation \mathcal{F} . Here, $\mathbf{m}_{1:t-1}$ denotes the accumulated mask features taken from stage 1 to stage $t-1$.

To a certain extent, the interleaved execution and mask information flow alleviate the problems in Cascade Mask R-CNN; however, these ideas still have limitations to be addressed. First, the sample inconsistency remains unsolved. Second, HTC is still constrained by multi-stage mask predictions and mask ensemble. It requires multiple ROI feature extractors, upsamplers, and predictors, and practically, they are resource-consuming.

4 The proposed SCNet

4.1 Sample Consistency

The proposed SCNet introduces sample consistency that ensures the consistency in the sample distribution at training and inference. Two versions of sample consistency are considered: naive and effective sample consistency. The naive sample consistency moves all the mask branches after the last box stage and the output of the last box stage is used for extracting mask features for all mask branches at both training and inference (Figure 3a). Although the sample consistency is attained, it still requires the repetition of computationally expensive operations, such as ROI feature extraction, feature upsampling, and mask prediction. Computational efficiency is an important measure in segmentation, which is usually used as a front-end task for many other tasks. To speed up the network, the effective sample consistency is proposed to use a single deep mask branch instead of multiple shallow ones (Figure 3b), which is used by default in SCNet. In detail, the common three 4-convolution mask branches are “stacked” to be a sequence of 12 consecutive convolution layers. Since the mask branches is deep, a skip connect is used after every two convolution layers. Effective sample consistency avoids the repetition of expensive operations since it relies on a single mask branch. Beside ensuring sample consistency and speeding up the network, the proposed method also addresses the problem of Cascade Mask R-CNN in that all the mask branches are isolated without direct connection, and the problem of mask predictions on intermediate noisy boxes.

4.2 Feature Relay and Global Context

Feature relay and global context strengthen the relationships among classifying, detecting and segmenting sub-tasks. Motivated by the observation that “implicit” mutual information between the box and mask branches improves the overall performance, the feature relay “explicitly” incorporates the box features with the mask features to improve the mask prediction. Feature relay exploits the relationship between detection and segmentation sub-tasks such that the box features provide the mask branch the prior for the mask prediction, and the mask prediction supervises (refines) the box features via back-propagation. This tightly coupled relationship between detection and segmentation sub-tasks leads to the performance gain. Figure 4 shows a detailed architecture of the feature relay module. In concrete, the output features of the box branch are first sliced to obtain the ones w.r.t. positive samples then fed into a fully connected layer to align box feature space with mask feature space. The box features, which are in vector-form, are reshaped to matrix-form and upsampled before being fused with the mask features by element-wise summation. It is noted that feature relay only fuses the box and mask features at the same stage since they share the common ROI locations. When feature relay is combined with sample consistency, it is only applied to the last stage, as shown in Figure 2c.

The global context branch takes as input the backbone features and outputs the multi-label predictions and global context features. Figure 5 shows the global context branch

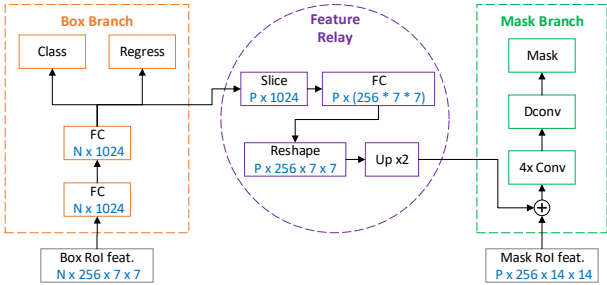


Figure 4: Architecture of feature relay. Here, “N” and “P” denotes the number of total samples and positive samples, respectively. “FC”, “ $\times 4$ Conv”, and “Dconv” denote fully connected layer, four consecutive convolution layers, and a deconvolution layer, respectively

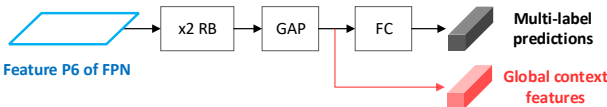


Figure 5: Global context branch takes the top-level features (P6) of FPN (Lin et al. 2017) as the input and produces multi-label predictions and global context features. Here, “ $\times 2$ RB” and “GAP” denotes two residual blocks and a global average pooling layer, respectively

on the FPN backbone features. First, the top-level features of FPN are fed into two consecutive residual blocks, followed by global average pooling. The pooled features are used in two sub-branches, which are multi-label classification and global context features. The multi-label predictions are supervised by all the known objects in the image, and the context features are used to fuse with box and mask features, as shown in Figure 3d.

4.3 Training

The proposed SCNet can be trained in an end-to-end manner using multi-task loss as follows:

$$\mathcal{L} = \sum_{t=1}^T \alpha_t (\mathcal{L}_t^{cls} + \mathcal{L}_t^{reg}) + \beta \mathcal{L}^{mask} + \gamma \mathcal{L}^{sema} + \lambda \mathcal{L}^{glbctx}. \quad (3)$$

Here, \mathcal{L}^{cls} , \mathcal{L}^{reg} , \mathcal{L}^{mask} , and \mathcal{L}^{sema} are the losses of classification, regression, mask prediction, and semantic prediction, respectively. The concrete loss types and loss weights (*i.e.*, α_t and γ) are referred to in (Chen et al. 2019a) without any modifications. Since effective sample consistency uses only one mask branch, the mask loss weight is re-weighted to equal the summation of stage-wise loss weights:

$$\beta = \sum_{t=1}^T \alpha_t. \quad (4)$$

Besides, SCNet introduce a new global context loss \mathcal{L}^{glbctx} , which performs multi-label classification and is implemented using binary cross entropy.

5 Experiments

5.1 Implementation Details

The default model consists of 3 cascading stages with the ResNet FPN (Lin et al. 2017) being the backbone network. The stage loss weights and semantic loss weight, which are adopted from (Chen et al. 2019a), are set to $\alpha = [1, 0.5, 0.25]$ and $\gamma = 0.2$, respectively. The global context loss weight is set to $\lambda = 3$.

In all experiments, the long edge and short edge of the images are resized to 1333 and 800, respectively, without changing the aspect ratio. No data augmentation is used except for standard horizontal image flipping. PyTorch (Paszke et al. 2017) and MMDetection (Chen et al. 2019b) are used for implementation. The models are trained with 8 GPUs with a batch size of 16 (two images per GPU) for 20 epochs using SGD optimizer. The learning rate is initialized to 0.02 and divided by 10 after 16 and 19 epochs, respectively. It takes about one day for the models to converge on 8 Tesla V100 GPUs.

During test time, object proposals are progressively refined by box branches of different stages. The final classification score for each detected box is obtained by averaging the scores of multiple classifiers, referred to in Cascade R-CNN (Cai and Vasconcelos 2018). Only the detected boxes with classification scores higher than a threshold of 0.001 are segmented by the mask branch.

Detection and segmentation results are evaluated with the standard COCO-style Average Precision (AP) metric. The runtime is measured on a single Tesla V100 GPU.

5.2 Benchmarking Results

The performance of SCNet is compared to that of recent state-of-the-art instance segmentation methods, including Cascade Mask R-CNN (Cai and Vasconcelos 2019) and Hybrid Task Cascade (HTC) (Chen et al. 2019a). For a fair comparison, the semantic branch, referred to in (Chen et al. 2019a), is adopted for all the cascade models. Besides, SCNet is also benchmarked with other non-cascade models, including Mask R-CNN (He et al. 2017) and PANet (Liu et al. 2018), LevelSet R-CNN (Homayounfar et al. 2020), BlendMask (Chen et al. 2020), BMask R-CNN (Cheng et al. 2020), and D2Det (Cao et al. 2020).

Table 1 reports the benchmarking results of the state-of-the-art segmentation methods. Overall, the cascade models show better box AP and mask AP than those of the non-cascade ones. Among cascade models, the proposed SCNet achieves the best performance in not only box AP and mask AP but also inference speed, irrespective of the backbone strength. In particular, with the default setting of backbone ResNet-50, the proposed SCNet achieves 1.3 and 2.3 points box AP and mask AP improvements, respectively. The mask AP at different IoU thresholds (AP_{50} , AP_{75}) and object scales (AP_S , AP_M , AP_L) are also consistently higher than other methods. Regarding inference speed, SCNet runs at 6.2 fps, which is 1.7 fps (38%) faster than Cascade Mask R-CNN and HTC. When applying better backbones of ResNet-101 or ResNeXt-101, SCNet also outperforms other methods among the benchmarking metrics, demonstrating the

Table 1: Benchmarking results between the proposed SCNet and other state-of-the-art methods on COCO test-dev. Here, AP and AP^{bb} are the mask AP and box AP, respectively. The semantic branch (Chen et al. 2019a) is used for all cascade models.

Type	Method	Backbone	AP	AP ₅₀	AP ₇₅	AP _S	AP _M	AP _L	AP ^{bb}	Speed (fps)
None-cascade methods	Mask R-CNN	ResNet-50	35.6	57.6	38.0	18.9	38.4	46.4	38.9	11.3
	PANet		36.6	58.0	39.9	16.3	38.1	52.4	41.2	-
	LevelSet R-CNN		36.4	-	-	-	-	-	-	-
	BlendMask		37.0	58.9	39.7	17.3	39.4	52.5	-	-
	BMask R-CNN		35.9	57.0	38.6	15.8	37.6	52.2	-	-
Cascade methods	D2Det	ResNet-101	40.2	61.5	43.7	-	-	-	45.4	-
	Cascade Mask R-CNN	ResNet-50	37.9	59.8	40.8	20.2	40.2	50.2	43.7	4.5
	HTC		38.5	60.1	41.7	20.4	40.6	51.2	43.6	4.5
	SCNet (ours)		40.2	62.3	43.4	22.4	42.8	53.4	45.0	6.2
	Cascade Mask R-CNN	ResNet-101	39.2	61.3	42.4	20.9	41.7	52.2	45.3	4.4
	HTC		39.7	61.8	43.0	20.9	42.4	53.0	45.1	4.4
	SCNet (ours)		41.3	63.9	44.8	22.7	44.1	55.2	46.4	5.8
	Cascade Mask R-CNN	ResNeXt-101	40.9	63.7	44.2	22.4	43.5	54.2	47.3	3.7
	HTC		41.3	63.9	44.8	22.7	44.0	54.7	47.2	3.7
	SCNet (ours)		42.7	65.7	46.4	24.1	45.7	56.3	48.3	4.6

Table 2: Ablation study of the proposed SCNet on COCO val, the baseline is Cascade Mask R-CNN (Cai and Vasconcelos 2019) with semantic (Chen et al. 2019a)

Cascade Mask R-CNN	Sample Consistency	Feature Relay	Global Context	AP	AP ₅₀	AP ₇₅	AP ^{bb}	Speed (fps)
✓				37.4	59.0	40.0	43.3	4.5
✓	✓			38.8	59.8	41.7	43.5	6.5
✓		✓		38.0	59.2	40.8	43.4	4.1
✓			✓	38.3	59.8	41.2	44.5	4.4
✓	✓	✓		39.0	60.0	41.9	43.7	6.3
✓	✓	✓	✓	39.8	61.4	42.7	44.6	6.2
Overall Improvement				+2.4	+2.4	+2.7	+1.3	+1.7

effectiveness of the proposed method. Qualitatively, Figure 6 shows the visual comparison of the proposed SCNet with other cascade models. It is clear that SCNet produces more accurate number of instances with better-segmented masks.

5.3 Ablation Study

Component-wise Analysis. To demonstrate the effectiveness of the proposed SCNet, a comprehensive component-wise analysis is performed, where different components are omitted. The results are reported in Table 2. Here, the baseline is Cascade Mask R-CNN (Cai and Vasconcelos 2019) with the semantic branch (Chen et al. 2019a) being applied, yielding the box AP and mask AP of 43.3 and 37.4, respectively. When sample consistency is ensured, the mask AP increases significantly to 38.8. The inference speed is also improved to 6.5 fps. When feature relay and global context are applied, the mask AP improvements are 0.6 and 0.9 points, respectively. When sample consistency and feature relay is combined, the mask AP increase from 38.8 to 39.0. The improvement of 0.2 points is because of the number of feature relay modules reduces from 3 to 1 when sample con-

Table 3: Comparison between naive and effective sample consistency (denoted as SC). Cascade Mask R-CNN is denoted as CM R-CNN.

CM R-CNN	Naive SC	Effective SC	AP	AP bb	Speed (fps)
✓			37.4	43.3	4.5
✓	✓		38.0	43.5	4.5
✓		✓	38.8	43.5	6.5

sistency is combined with feature relay. The combination of all components brings the best mask and box AP of 39.8 and 33.6, respectively. Overall, SCNet achieves respectively 2.4 points, 1.3 points and 1.7 fps improvements in terms of mask AP, box AP, and inference speed in comparison with the baseline.

Sample Consistency. To demonstrate the effectiveness of sample consistency, the experiments of the naive and effective sample consistency are reported, as shown in Table 3. When naive sample consistency is applied, the mask AP is improved from 37.4 to 38.0 and the speed is kept un-

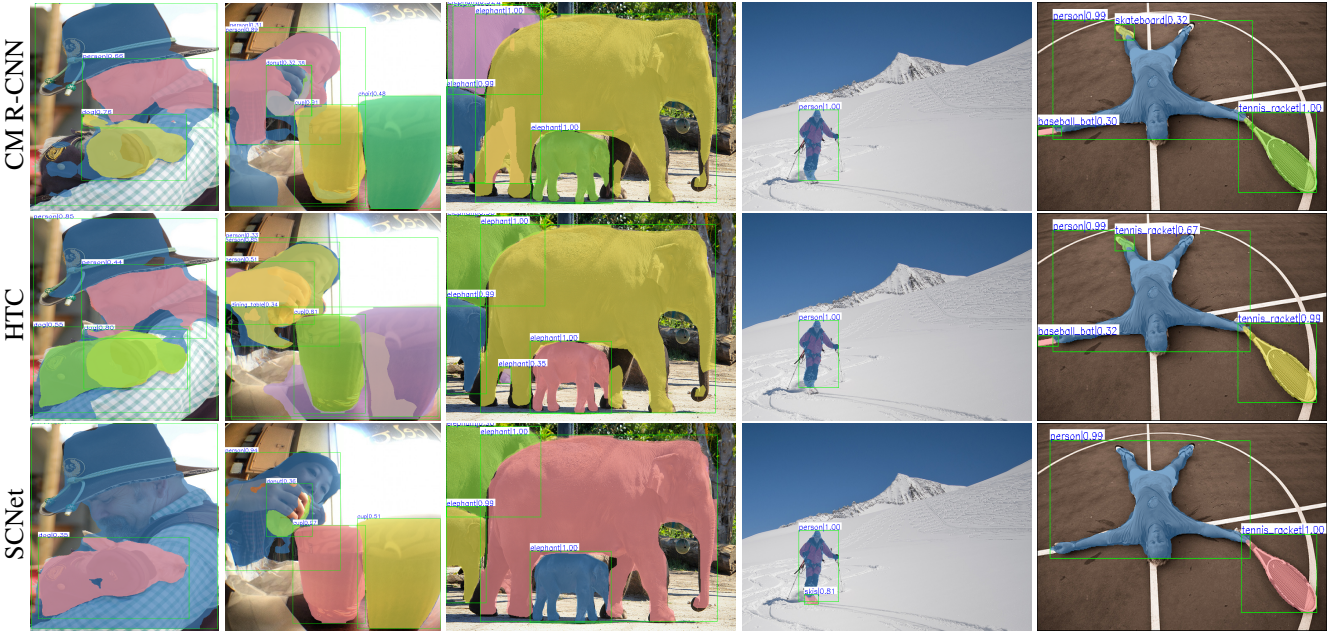


Figure 6: Qualitative comparison between the proposed SCNet and other methods on COCO val (zoom-in for best view). The proposed SCNet produces more accurate the number of instances with better segmented masks.

Table 4: Ablation study on Feature Relay.

Model	Feature Relay	AP	AP ^{bb}	Speed (fps)
Mask R-CNN	N	35.1	38.4	7.7
	Y	35.7	38.3	7.4
Cascade Mask R-CNN	N	37.4	43.3	4.5
	Y	38.0	43.4	4.1

changed of 4.5 fps. This is because the naive sample consistency still requires multiple mask branches. When effective sample consistency is used, both mask AP and inference speed are significantly improved. The inference speed is faster since it avoid the repetition of expensive operations through stages. The better mask AP shows that using a single deep network is more beneficial compared to using multiple shallow ones.

Feature Relay. The feature relay fuses the adapted box features with the mask features to achieves better mask prediction. feature relay can be seamlessly applied to common segmentation methods, such as Mask R-CNN and Cascade R-CNN. Table 4 shows that feature relay can improve mask AP by 0.6 points in both Mask R-CNN and Cascade Mask R-CNN with marginal computational overhead. The box AP is comparable to the baseline since the feature relay aims to improve the mask predictions only.

Global Context. The effectiveness of global context branch under different settings is studied in Table 5. Here, when the global context is not used (λ is “None”), SCNet achieves the mask AP of 39.0. When the global context branch is used but the loss weight is set to 0, the mask

Table 5: Ablation study of the global context loss weight λ .

λ	AP	AP ₅₀	AP ₇₅	AP _S	AP _M	AP _L	AP ^{bb}
None	39.0	60.0	42.0	20.2	41.8	54.5	43.7
0	39.6	61.3	42.6	21.9	42.7	54.8	44.4
1	39.6	61.3	42.6	21.9	42.8	55.0	44.5
2	39.7	61.2	42.8	21.7	42.9	55.1	44.6
3	39.8	61.4	42.7	22.1	43.0	54.5	44.6
5	39.6	61.3	42.6	21.8	42.7	55.0	44.5

AP increase to 39.6. The performance increases when the loss weight is greater than 0 and is not sensitive to the loss weight. Setting the weight to 3 achieves the best overall performance, which is 0.8 points mask AP improvement.

6 Conclusion

This paper introduces SCNet, a simple yet effective architecture for instance segmentation. The proposed SCNet ensures sample consistency of IoU distribution in training and inference while speeding up the network. Furthermore, SCNet strengthens the relationships of the sub-tasks by feature relay and global context. Extensive experiments on the standard COCO dataset show the effectiveness of the proposed method in multiple evaluation metrics. In concrete, while running at a faster inference speed, the proposed SCNet improves the Average Precision of the box and mask predictions by respectively 1.3 and 2.3 points compared to the strong Cascade Mask R-CNN baseline.

Acknowledgement

This work was partly supported by Institute for Information & communications Technology Planning & Evaluation (IITP) grant funded by the Korea government (MSIP) (No. 2018-0-00198), Object information extraction and real-to-virtual mapping based AR technology) and partly supported by Institute for Information & communications Technology Planning & Evaluation(IITP) grant funded by the Korea government(MSIT) (2017-0-01780, The technology development for event recognition/relational reasoning and learning knowledge based system for video understanding).

References

- Arnab, A.; and Torr, P. H. 2016. Bottom-up instance segmentation using deep higher-order crfs. *arXiv:1609.02583*.
- Bai, M.; and Urtasun, R. 2017. Deep Watershed Transform for Instance Segmentation. In *CVPR*.
- Cai, Z.; and Vasconcelos, N. 2018. Cascade R-CNN: Delving Into High Quality Object Detection. In *CVPR*.
- Cai, Z.; and Vasconcelos, N. 2019. Cascade R-CNN: High Quality Object Detection and Instance Segmentation. *arXiv:1906.09756*.
- Cao, J.; Cholakkal, H.; Anwer, R. M.; Khan, F. S.; Pang, Y.; and Shao, L. 2020. D2Det: Towards High Quality Object Detection and Instance Segmentation. In *CVPR*.
- Cao, Y.; Xu, J.; Lin, S.; Wei, F.; and Hu, H. 2019. Gcnet: Non-local networks meet squeeze-excitation networks and beyond. In *ICCV Workshops*.
- Chen, H.; Sun, K.; Tian, Z.; Shen, C.; Huang, Y.; and Yan, Y. 2020. BlendMask: Top-down meets bottom-up for instance segmentation. In *CVPR*.
- Chen, K.; Pang, J.; Wang, J.; Xiong, Y.; Li, X.; Sun, S.; Feng, W.; Liu, Z.; Shi, J.; Ouyang, W.; et al. 2019a. Hybrid task cascade for instance segmentation. In *CVPR*.
- Chen, K.; Wang, J.; Pang, J.; Cao, Y.; Xiong, Y.; Li, X.; Sun, S.; Feng, W.; Liu, Z.; Xu, J.; Zhang, Z.; Cheng, D.; Zhu, C.; Cheng, T.; Zhao, Q.; Li, B.; Lu, X.; Zhu, R.; Wu, Y.; Dai, J.; Wang, J.; Shi, J.; Ouyang, W.; Loy, C. C.; and Lin, D. 2019b. MMDetection: Open MMLab Detection Toolbox and Benchmark. *arXiv:1906.07155*.
- Cheng, T.; Wang, X.; Huang, L.; and Liu, W. 2020. Boundary-preserving mask R-CNN. In *ECCV*.
- Dai, J.; He, K.; Li, Y.; Ren, S.; and Sun, J. 2016. Instance-sensitive fully convolutional networks. In *ECCV*.
- Dai, J.; He, K.; and Sun, J. 2016. Instance-Aware Semantic Segmentation via Multi-Task Network Cascades. In *CVPR*.
- Danielczuk, M.; Matl, M.; Gupta, S.; Li, A.; Lee, A.; Mahler, J.; and Goldberg, K. 2019. Segmenting unknown 3d objects from real depth images using mask r-cnn trained on synthetic data. In *ICRA*.
- Girshick, R. 2015. Fast r-cnn. In *ICCV*.
- He, K.; Gkioxari, G.; Dollar, P.; and Girshick, R. 2017. Mask R-CNN. In *ICCV*.
- Homayounfar, N.; Xiong, Y.; Liang, J.; Ma, W.-C.; and Urtasun, R. 2020. LevelSet R-CNN: A Deep Variational Method for Instance Segmentation. In *ECCV*.
- Kim, J.; Ma, M.; Kim, K.; Kim, S.; and Yoo, C. D. 2019. Progressive attention memory network for movie story question answering. In *CVPR*.
- Kim, J.; Ma, M.; Pham, T.; Kim, K.; and Yoo, C. D. 2020. Modality Shifting Attention Network for Multi-Modal Video Question Answering. In *CVPR*.
- Li, Y.; Qi, H.; Dai, J.; Ji, X.; and Wei, Y. 2017. Fully Convolutional Instance-Aware Semantic Segmentation. In *CVPR*.
- Lin, T.-Y.; Dollar, P.; Girshick, R.; He, K.; Hariharan, B.; and Belongie, S. 2017. Feature Pyramid Networks for Object Detection. In *CVPR*.
- Lin, T.-Y.; Maire, M.; Belongie, S.; Hays, J.; Perona, P.; Ramanan, D.; Dollár, P.; and Zitnick, C. L. 2014. Microsoft coco: Common objects in context. In *ECCV*.
- Liu, S.; Jia, J.; Fidler, S.; and Urtasun, R. 2017. SGN: Sequential Grouping Networks for Instance Segmentation. In *ICCV*.
- Liu, S.; Qi, L.; Qin, H.; Shi, J.; and Jia, J. 2018. Path Aggregation Network for Instance Segmentation. In *CVPR*.
- Long, J.; Shelhamer, E.; and Darrell, T. 2015. Fully Convolutional Networks for Semantic Segmentation. In *CVPR*.
- Mao, T.; Zhang, W.; He, H.; Lin, Y.; Kale, V.; Stein, A.; and Kostic, Z. 2018. AIC2018 Report: Traffic Surveillance Research. In *CVPRW*.
- Neven, D.; De Brabandere, B.; Georgoulis, S.; Proesmans, M.; and Van Gool, L. 2018. Towards end-to-end lane detection: an instance segmentation approach. In *2018 IEEE Intelligent Vehicles Symposium (IV)*.
- Paszke, A.; Gross, S.; Chintala, S.; Chanan, G.; Yang, E.; DeVito, Z.; Lin, Z.; Desmaison, A.; Antiga, L.; and Lerer, A. 2017. Automatic differentiation in PyTorch. In *NIPS-W*.
- Pathak, D.; Shentu, Y.; Chen, D.; Agrawal, P.; Darrell, T.; Levine, S.; and Malik, J. 2018. Learning instance segmentation by interaction. In *CVPRW*.
- Peng, C.; Zhang, X.; Yu, G.; Luo, G.; and Sun, J. 2017. Large Kernel Matters—Improve Semantic Segmentation by Global Convolutional Network. In *CVPR*.
- Pinheiro, P. O.; Collobert, R.; and Dollár, P. 2015. Learning to segment object candidates. In *NIPS*.
- Pinheiro, P. O.; Lin, T.-Y.; Collobert, R.; and Dollár, P. 2016. Learning to refine object segments. In *ECCV*.
- Qiao, S.; Chen, L.-C.; and Yuille, A. 2020. DetectoRS: Detecting Objects with Recursive Feature Pyramid and Switchable Atrous Convolution. *arXiv:2006.02334*.
- Ren, S.; He, K.; Girshick, R.; and Sun, J. 2015. Faster R-CNN: Towards Real-Time Object Detection with Region Proposal Networks. In *NIPS*.
- Tian, Z.; Shen, C.; and Chen, H. 2020. Conditional Convolutions for Instance Segmentation. In *ECCV*.

Vu, T.; Jang, H.; Pham, T. X.; and Yoo, C. 2019. Cascade RPN: Delving into High-Quality Region Proposal Network with Adaptive Convolution. In *NeurIPS*.

Wang, X.; Girshick, R.; Gupta, A.; and He, K. 2018. Non-local neural networks. In *CVPR*.

Wang, X.; Kong, T.; Shen, C.; Jiang, Y.; and Li, L. 2020. SOLO: Segmenting Objects by Locations. In *ECCV*.

Xie, E.; Sun, P.; Song, X.; Wang, W.; Liu, X.; Liang, D.; Shen, C.; and Luo, P. 2020. Polarmask: Single shot instance segmentation with polar representation. In *CVPR*.

Zhang, Y.; Song, B.; Du, X.; and Guizani, M. 2018. Vehicle tracking using surveillance with multimodal data fusion. *IEEE Transactions on Intelligent Transportation Systems* .

Zhang, Z.; Fidler, S.; and Urtasun, R. 2016. Instance-level segmentation for autonomous driving with deep densely connected mrfs. In *CVPR*.

Zhang, Z.; Schwing, A. G.; Fidler, S.; and Urtasun, R. 2015. Monocular Object Instance Segmentation and Depth Ordering With CNNs. In *ICCV*.